Published in IET Radar, Sonar and Navigation
Received on 15th October 2012
Revised on 19th January 2013
Accepted on 18th February 2013
doi: 10.1049/iet-rsn.2012.0300

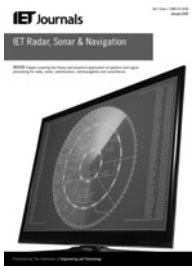

ISSN 1751-8784

Reconfigurable sum–difference pattern by means of parasitic elements for forward-looking monopulse radar

Paolo Rocca, Massimo Donelli, Giacomo Oliveri, Federico Viani, Andrea Massa

ELEDIA Research Center, Department of Information Engineering and Computer Science, University of Trento, Via Sommarive 5, 38123 Trento, Italy
E-mail: andrea.massa@ing.unitn.it

Abstract: This study describes the design of forward-looking monopulse arrays able to reconfigure the radiation pattern from the sum mode to the difference one by electronically switching a set of parasitic dipoles placed in front of a driven array of radiating dipoles. The antenna architecture is synthesised by optimising the geometric parameters of the passive elements, namely their positions and lengths. The generation of the difference beam is yielded by imposing a phase displacement of π to the excitations of half active array and activating the parasitic array by turning-on the switches that partition their lengths. As for the sum pattern, the effect of the parasitic dipoles is made negligible by turning-off the switches. A set of representative results is reported and discussed to show the effectiveness of the proposed approach.

1 Introduction

Antennas able to generate sum and difference patterns can be profitably exploited as monopulse radar trackers to locate and track the position of a moving target [1, 2] in a wide range of air-borne and terrestrial applications. More recently, sum and difference patterns have been also used in automotive radars [3] and radio-frequency identification ('RFID') readers [4] by orienting the two beams at broadside to detect the presence of a car along the forward direction or to narrow the angular extent of the RFID interrogation zone, respectively.

Usually, sum and difference patterns are generated by means of reflector antennas with multiple feeds or arrays of radiating elements [1]. This latter solution is nowadays preferred because of the larger number of degrees of freedom available in the design process, the possibility to electronically steer the radiation pattern, the compact realisation and the possibility to conform the array to the vehicle structure. However, the synthesis of two optimal beams still represents the main limitation to the diffusion of such radar systems because of the high complexity of the underlying array architecture. Therefore several strategies have been proposed to reduce the number of control points of the feeding network ranging from the generation of sub-optimal beams by aggregating the elements into clusters (i.e. the sub-arraying technique) [5–9] up to the use of common amplitude weights [10, 11].

In this work, a reconfigurable array for forward-looking monopulse applications able to generate broadside sum and difference patterns by means of a relatively inexpensive antenna structure is proposed. The antenna is made of an active array and a passive one placed in front of the driven elements as pictorially shown in Fig. 1. The dipoles of the passive array are divided into small segments ($<(\lambda/4)$) by placing a set of on–off switches along the wires of the dipoles. From an operative point of view, the sum beam [12] is generated by independently controlling the symmetric amplitude excitations of the active elements and turning-off the switches, whereas the difference one is obtained by introducing a phase displacement of π to the elements of half array and short-circuiting the switches such that they interact with the received signal. The position and the length of the parasitic dipoles are optimised by means of an evolutionary algorithm [13] to synthesise a compromise difference beam close as much as possible to an optimal/reference one with narrow beamwidth, deep slope along the boresight direction and low secondary lobes. Although the use of radio-frequency (RF) switches certainly causes an increment of the antenna complexity, it allows one to avoid mechanical positioning systems for the movement of the parasitic array [14]. It is important to observe that in [14], the possibility of reconfiguring the pattern from a pencil to a flat-topped broadside beam has been investigated without any need of real-time reconfigurability.

Since the distributions providing the two 'optimal' beams (e.g. Taylor [15] and Bayliss [16] patterns) have similar shape along the tail of the array, while they differ in the central part [10, 11], it is expected that, starting from an anti-symmetric set of Taylor excitations for the active array, the generation of a sub-optimal difference pattern can be obtained with a set of parasitic elements. Accordingly, the synthesis of reconfigurable arrays by means of parasitic dipoles, previously considered to mechanically switch between a pencil beam and a flat-topped beam [14], is here

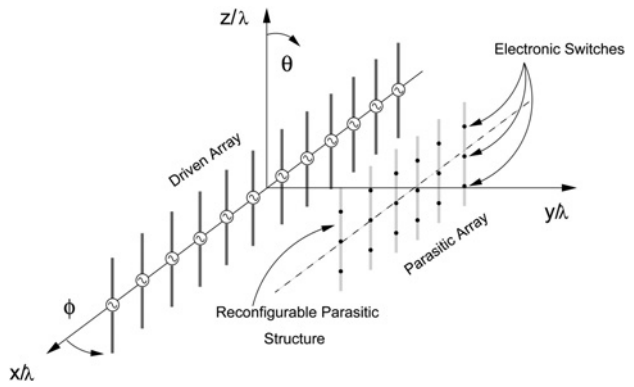

Fig. 1 *Visual representation of the composite antenna*

proposed to electronically reconfigure the radiation pattern of a forward-looking monopulse radar from a sum pattern to a difference one. Although alternative optimal solutions providing sum [17, 18] and difference [19, 20] beams are available, Taylor and Bayliss distributions have been considered in this work since they have been widely adopted in monopulse array design [1, 2].

The paper is organised as follows. The array synthesis problem is mathematically formulated in Section 2, where the optimisation strategy is presented, as well. A set of selected results is reported in Section 3 to point out the potentialities of the proposed approach. Eventually, some conclusions are drawn (Section 4).

2 Mathematical formulation

Let us consider a linear array of $N = 2M$ dipoles located on the x-axis and oriented along the z-direction. The radiated electric field is equal to

$$E(\theta,\ \phi) = F(\theta) \sum_{m=-M,\ m\neq 0}^{M} I_m \mathrm{e}^{\mathrm{j}k\left(m-(\mathrm{sgn}(m))/2\right)d\sin\theta\cos\phi} \quad (1)$$

where I_m, $m = \pm 1, \ldots, \pm M$, is the set of array excitations, $k = (2\pi/\lambda)$ is the wave number, λ being the free-space wavelength, sgn$(\cdot)$ is the sign function and d is the inter-element distance. Moreover, (θ, ϕ) denotes the angular direction (Fig. 1) and $F(\theta)$ is the element factor of a finite dipole of length l [21]

$$F(\theta) = \frac{\cos\left((\pi l\cos\theta)/2\right) - \cos\left((\pi l)/2\right)}{\sin\theta} \quad (2)$$

When the distribution of the excitations is characterised by an even symmetry, $I_{-m} = I_m$, $m = 1, \ldots, M$, as for the Taylor distribution (Fig. 2*a*), the field models a sum pattern (Fig. 2*b*) that, by virtue of the Euler's trigonometric identities, can be represented in terms of a cosine expansion

$$E^{\Sigma}(\theta,\ \phi) = 2F(\theta)\sum_{m=1}^{M} I_m^{\Sigma}\cos\left[k\left(m-\frac{1}{2}\right)d\sin\theta\cos\phi\right] \quad (3)$$

where only half-elements are considered because of the symmetry of the excitation weights. When the values I_m^{Σ}, $m = 1, \ldots, M$ are set to the Taylor distribution [15], the pattern $E^{\Sigma}(\theta, \phi)$ turns out to be the best trade-off between main-lobe beamwidth, sidelobe level and peak directivity. These features are very attractive for monopulse radars

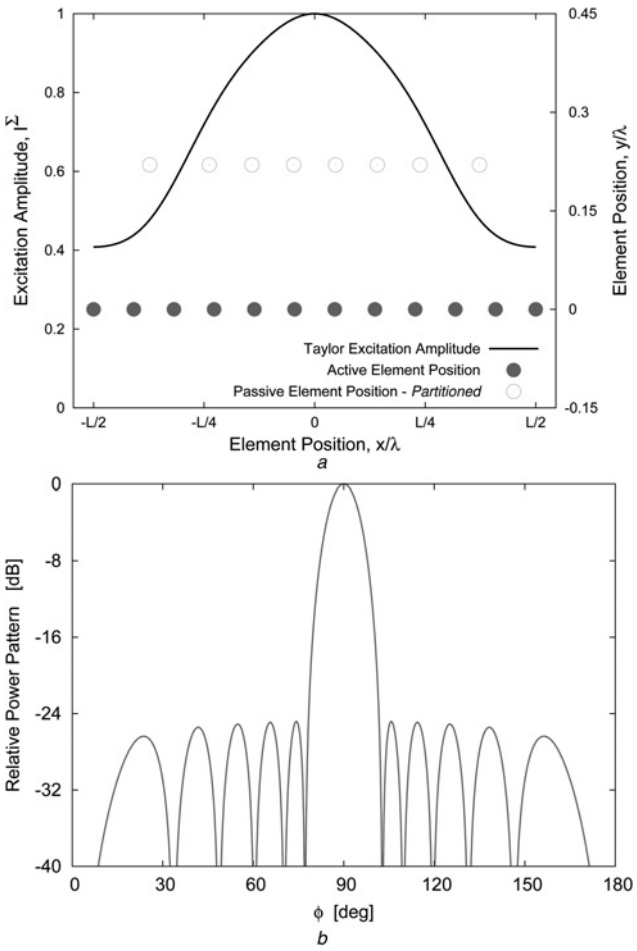

Fig. 2 *Optimal sum distribution*

a Excitation distribution
b Radiated pattern

because of the need to intercept the signal from the target (i.e. high directivity) with a good spatial resolution (i.e. narrow beamwidth) also avoiding interferences and reducing the noise (i.e. low secondary lobes) at the same time.

To generate a difference pattern, an odd distribution of the excitations is required: $I_{-m} = -I_m$, $m = 1, \ldots, M$. Such a distribution can be obtained by taking symmetric coefficients and imposing a phase displacement of π to half-elements since $-I_m = I_m \mathrm{e}^{\mathrm{j}\pi}$. The radiated field can be then represented as a summation of sine functions

$$E^{\Delta}(\theta,\ \phi) = 2\mathrm{j}F(\theta)\sum_{m=1}^{M} I_m^{\Delta}\sin\left[k\left(m-\frac{1}{2}\right)d\sin\theta\cos\phi\right] \quad (4)$$

However, if $I_m^{\Delta} = I_m^{\Sigma}$, $m = 1, \ldots, M$ (Fig. 3*a*), the synthesised pattern presents high secondary lobes as shown in Fig. 3*b*. To yield an 'optimal' difference beam with the best trade-off between main-lobe beamwidth, sidelobe level and slope along the boresight direction, Bayliss coefficients [12] are usually adopted (Fig. 4).

To avoid the generally undesired [22] use of a couple of dedicated and independent feed networks or reconfigurable amplitudes, the following architecture is taken into account. The active elements are first feed to generate an 'optimal' sum pattern (i.e. $I_m = I_m^{\Sigma}$, $m = 1, \ldots, M$), whereas the difference pattern is yielded by adding a phase shift of π to the excitations of half active elements and placing on a line

doi: 10.1049/iet-rsn.2012.0300

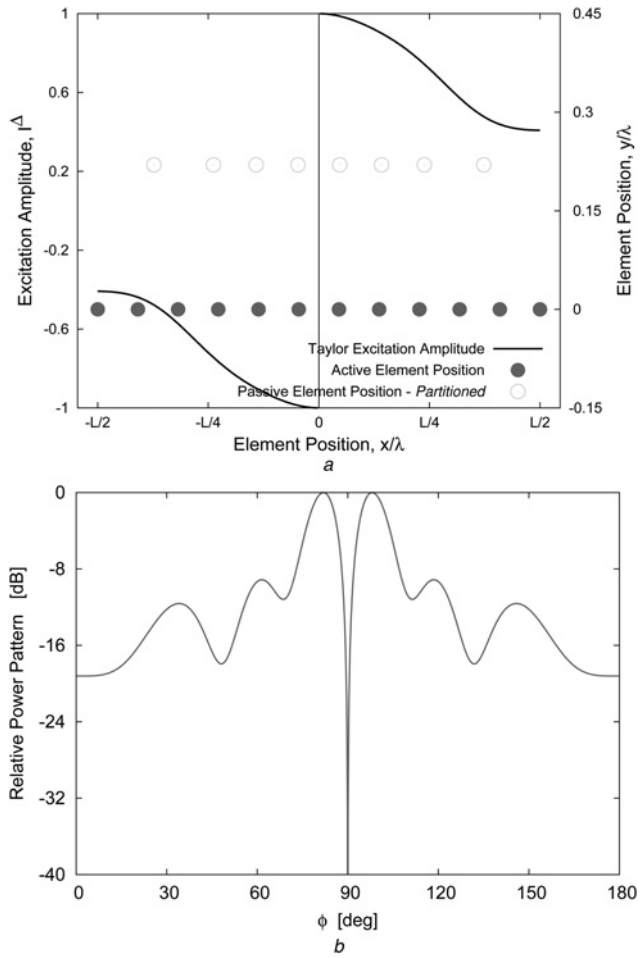

Fig. 3 *Anti-symmetric optimal sum distribution*
a Excitation distribution
b Radiated pattern

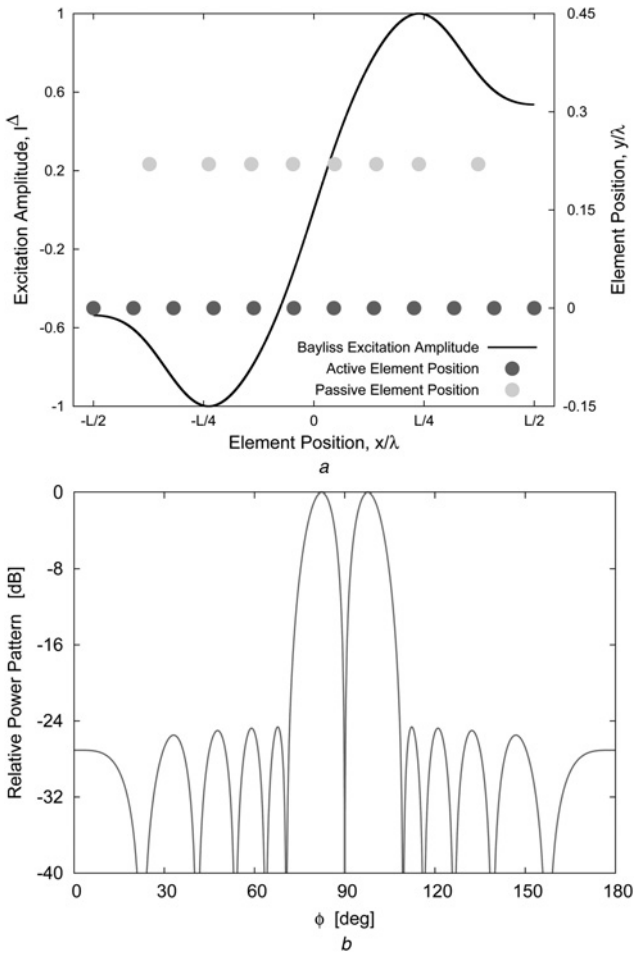

Fig. 4 *Optimal difference distribution*
a Excitation distribution
b Radiated pattern

parallel to the x-axis in front of the driven array, a passive array of $2P$ ($P < M$) parasitic dipoles oriented as the active ones (Fig. 5). Mathematically, the radiated field assumes the following expression

$$E^{\Delta}_{pa}(\theta, \phi) = 2\mathrm{j}F(\theta)\sum_{m=1}^{M}\hat{I}^{\Sigma}_{m}\sin\left[k\left(m-\frac{1}{2}\right)d\sin\theta\cos\phi\right] + \sum_{p=1}^{2P}\hat{I}^{pa}_{p}\mathrm{e}^{\mathrm{j}k\sin\theta\{x_p\cos\phi+\Delta y\sin\phi\}}F_{p}(\theta) \quad (5)$$

where $\hat{I}^{\Sigma}_{m}$, $m = 1, \ldots, M$, and $\hat{I}^{pa}_{p}$, $p = 1, \ldots, 2P$, are the complex amplitudes of the array elements determined by solving the system of linear equations $\underline{\boldsymbol{I}} = [\boldsymbol{Z}]^{-1}\underline{\boldsymbol{V}}$ [23], where

- $\underline{\boldsymbol{V}}$ is the vector of known voltages applied to the driven elements, whereas $\boldsymbol{V}_p = 0$, $p = 1, \ldots, 2P$, for passive elements;
- $\underline{\boldsymbol{I}}$ is the vector of the unknown current excitations on both driven and parasitic elements, $\underline{\boldsymbol{I}} = \left\{\hat{I}^{\Sigma}_{1}, \ldots, \hat{I}^{\Sigma}_{M}, \hat{I}^{pa}_{1}, \ldots, \hat{I}^{pa}_{2P}\right\}$;
- $[\boldsymbol{Z}]$ in the impedance matrix where the self-impedances $\boldsymbol{Z}_{ii}$ and the mutual impedances $\boldsymbol{Z}_{ij}$ $(i \neq j)$ are computed according to [24] for fixed values of $\underline{\boldsymbol{h}}$, Δy and $\underline{\boldsymbol{x}}$.

Moreover, $F_p(\theta)$ is the elements factor of the pth parasitic element given by (2) when $l = h_p$, $p = 1, \ldots, 2P$.

Since the passive array is symmetric, as well, the parameters to be determined turn out to be the distance Δy from the driven array (Fig. 5*a*), the element positions along the x-axis, $\underline{\boldsymbol{x}} = \left\{x_p, p = 1, \ldots, P\right\}$ (Fig. 5*a*), and the length $\underline{\boldsymbol{h}} = \left\{h_p, p = 1, \ldots, P\right\}$ (Fig. 5*b*) of the parasitic dipoles. Towards this end, the following cost function

$$\Psi(\underline{h}, \Delta y, \underline{x}) = \frac{\int_0^{\pi}\left|\left|E^{\Delta}_{pa}(\theta, \phi)\right|^2_{\theta=(\pi/2)} - \left|E^{\Delta}_{\mathrm{opt}}(\theta, \phi)\right|^2_{\theta=(\pi/2)}\right|\mathrm{d}\phi}{\int_0^{\pi}\left|E^{\Delta}_{\mathrm{opt}}(\theta, \phi)\right|^2_{\theta=(\pi/2)}\mathrm{d}\phi} \quad (6)$$

quantifying the matching of the radiated pattern $E^{\Delta}_{pa}(\theta, \phi)$ to a reference/optimal one $E^{\Delta}_{\mathrm{opt}}(\theta, \phi)$ in the azimuthal plane (i.e. $\theta = (\pi/2)$), as required in forward-looking radar systems, is then minimised by means of a particle swarm optimisation ('PSO')-based approach [13] pictorially described in the flowchart shown in Fig. 6 and summarised in the following:

Step 0: Selection of the optimal sum mode: For a given number of elements N and a suitable spacing d, the values

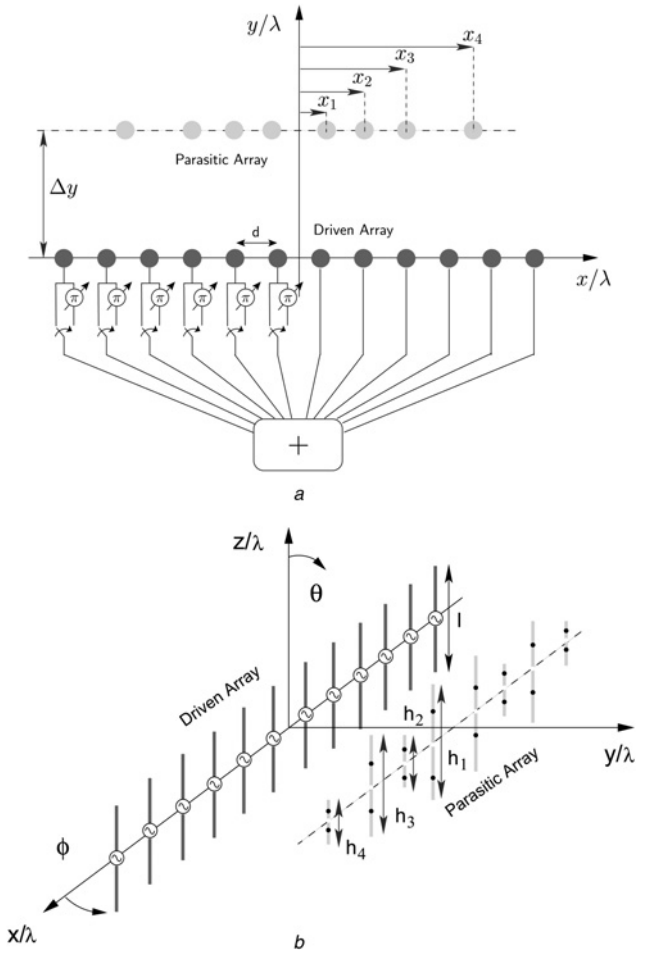

Fig. 5 *Sketch of the antenna architecture*

a Top view
b Three-dimensional view

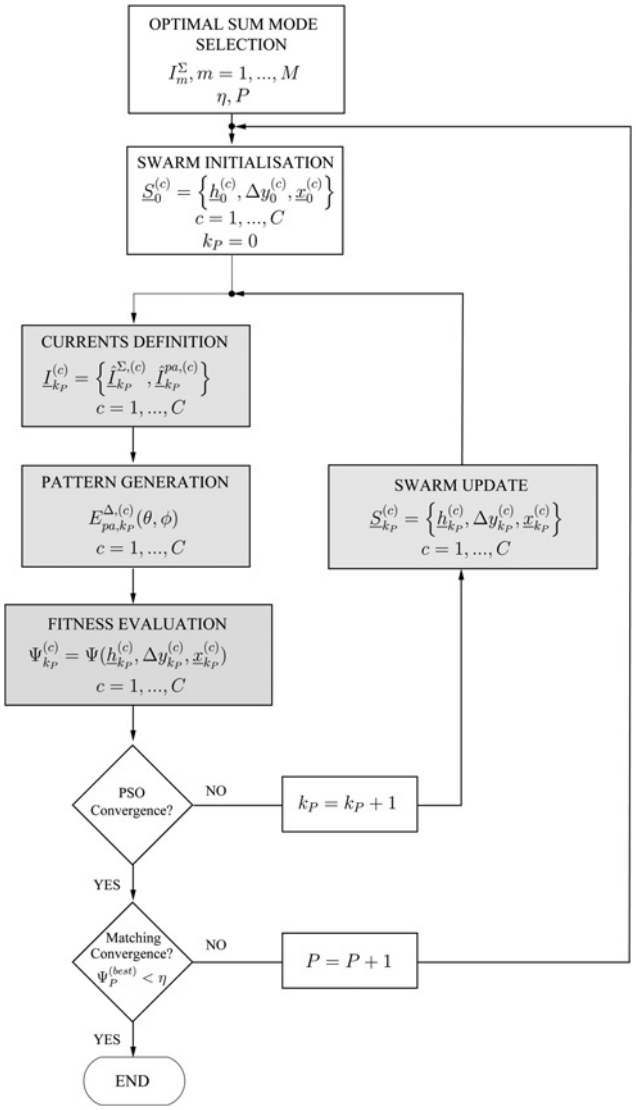

Fig. 6 *Flowchart of the antenna synthesis*

of the currents on the driven elements I_m^{Σ}, $m = 1,\ldots, M = (N/2)$ are set to generate an optimal sum pattern [15]. Moreover, an initial value for the number of parasitic elements P and a threshold η on the required matching performance (6) are chosen.

Step 1: *Swarm initialisation*: At the initialisation ($k_p = 0$), the values of the unknowns (i.e. the lengths, $\underline{\boldsymbol{h}}$, and the positions, Δy, $\underline{\boldsymbol{x}}$, of the parasitic elements) are randomly initialised for each particle of the swarm $\underline{\boldsymbol{S}}_{k_P}^{(u)} = \left\{\underline{\boldsymbol{h}}_{k_P}^{(u)}, \Delta y_{k_P}^{(u)}, \underline{\boldsymbol{x}}_{k_P}^{(u)}\right\}$, $u = 1,\ldots,U$, U being the swarm size.

Step 2: *PSO-based optimisation loop*: The synthesis of the difference pattern is then yielded through the following iterative optimisation:

Step 2a: *Definition of the currents on the elements of the antenna*: The entries of the impedance matrix $[\boldsymbol{Z}]_{k_P}^{(u)}$ are computed and the values of the currents $\underline{\boldsymbol{I}}_{k_P}^{(u)} = \left\{\hat{I}_{1,k_P}^{\Sigma,(u)}, \ldots, \hat{I}_{M,k_P}^{\Sigma,(u)}, \hat{I}_{1,k_P}^{pa,(u)}, \ldots, \hat{I}_{2P,k_P}^{pa,(u)}\right\}$, $u = 1,\ldots,U$ are determined according to [14, 23].

Step 2b: *Generation of the radiated field*: The radiated difference pattern is computed as in (5).

Step 2c: *Fitness evaluation*: The cost function is evaluated for each trial solution of the swarm, $\Psi_{k_P}^{(u)} = \Psi\left(\underline{\boldsymbol{h}}_{k_P}^{(u)}, \Delta y_{k_P}^{(u)}, \underline{\boldsymbol{x}}_{k_P}^{(u)}\right)$. Afterwards, if the convergence criterion based on either a maximum number of iterations K or on the stagnation of the optimal value of the cost function [i.e. $\Psi\left(\underline{\boldsymbol{S}}_{k_P}^{(\text{best})}\right)$]

$$\frac{\left|K_{\text{window}}\Psi\left(\underline{\boldsymbol{S}}_{k_P}^{(\text{best})}\right) - \sum_{q=1}^{K_{\text{window}}}\Psi\left(\underline{\boldsymbol{S}}_{k_P-q}^{(\text{best})}\right)\right|}{\Psi\left(\underline{\boldsymbol{S}}_{k_P}^{(\text{best})}\right)} \leq \xi \qquad (7)$$

being $\underline{\boldsymbol{S}}_{k_P}^{(\text{best})} = \arg\left\{\min_{u=1,\ldots,U}\left[\Psi_{k_P}^{(u)}\right]\right\}$, then $\underline{\boldsymbol{S}}_{P}^{(\text{best})} = \underline{\boldsymbol{S}}_{k_P}^{(\text{best})}$ and go to Step 3. Otherwise, go to Step 2d. The stopping rule (7) is applied for $k_p \geq K_{\text{window}}$ and when satisfied means that the fitness of the optimal solution has not changed of at least ξ, being ξ a user-defined numerical threshold, within a fixed number of K_{window} iterations.

Step 2d: *Swarm update*: The iteration index is updated, $k_p \leftarrow k_p + 1$, and U new trial solutions are defined by applying the evolutionary operators of the PSO, namely the velocity update and the position update [13], to the particles of the swarm.

Step 3: *Pattern matching evaluation*: Whether $\Psi_P^{(\text{best})} = \Psi\left(\underline{\boldsymbol{S}}_P^{(\text{best})}\right) < \eta$, then stop. Otherwise, the number of parasitic elements is increased, $P \leftarrow P + 1$, and then go Step 1.

With reference to the array architecture corresponding to the convergence solution $\underline{\boldsymbol{S}}_P^{(\text{best})}$, the antenna operates electronically as follows. The sum pattern is generated by

doi: 10.1049/iet-rsn.2012.0300

Table 1 'Reference excitations' – optimal excitations generating a Taylor sum pattern with SLL = –25 dB and $\bar{n} = 4$ [15] and a Bayliss difference pattern with SLL = –25 dB and $\bar{n} = 4$ [16]

m	I_m^{Σ}	I_n^{Δ}
1	0.381	0.289
2	0.413	0.511
3	0.475	0.675
4	0.561	0.824
5	0.661	0.951
6	0.764	1.000
7	0.856	0.935
8	0.928	0.762
9	0.976	0.503
10	1.000	0.177

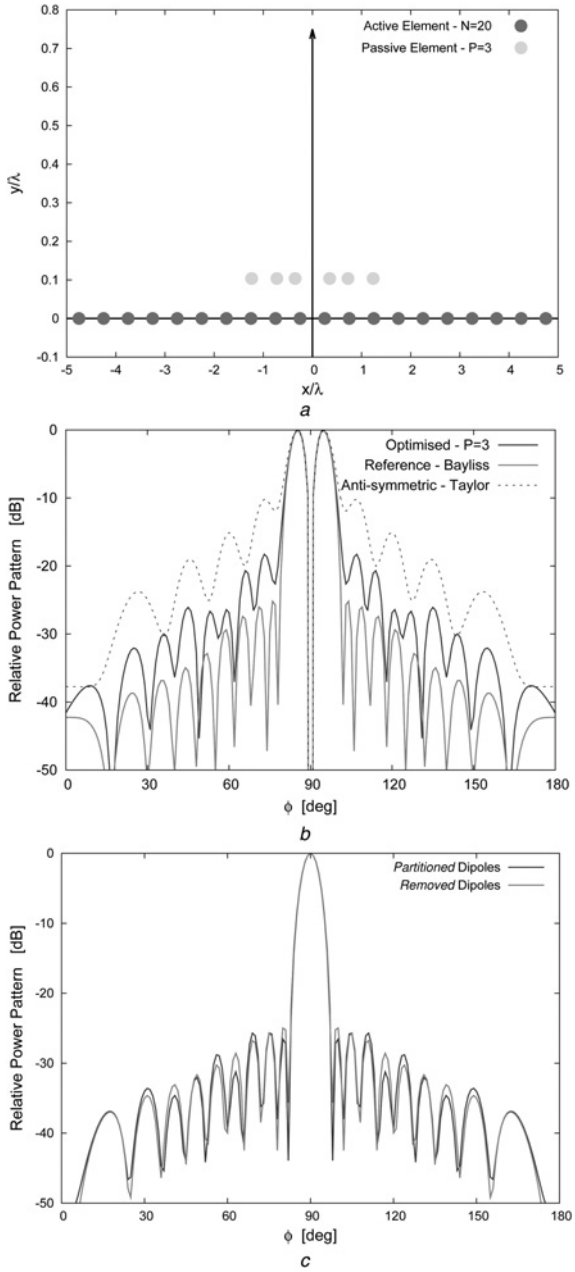

Fig. 7 *PSO-optimised antenna architecture and its operation in sum mode and difference mode when P =3*

a PSO-optimised antenna architecture
b Radiated difference beam
c Radiated sum beam

feeding the active array with symmetric static excitations (i.e. all the array elements radiate in phase) and de-activating the parasitic array by switching-off the RF switches [25], namely either RF- P-type, Intrinsic, N-type (PIN) diodes or RF-microelectromechanical system [26, 27]. On the other hand, the difference pattern is yielded by introducing a phase displacement of π to the elements of half of the active array and short-circuiting the switches of the parasitic structure.

3 Numerical validation

In order to assess the effectiveness of the proposed approach, let us consider an active array of $N = 20$ half-wavelength (i.e. $l = (\lambda/2)$) dipoles equally spaced by $d = (\lambda/2)$. Taylor excitations [15], I_m^{Σ}, $m = 1,\ldots, M$ (Table 1), have been assumed to provide an optimal sum mode with side lobe level (SLL) = −25 dB and $\bar{n} = 4$. The optimal excitations generating the reference difference pattern I_m^{Δ}, $m = 1,\ldots, M$ have been instead chosen to afford a Bayliss pattern [16] with SLL = −25 dB and $\bar{n} = 4$ (Table 1). The length h_p, $p = 1, \ldots, P$ of the dipoles of the passive array has been partitioned in four segment by placing two on–off switches, one for each arm of the dipole wires (Fig. 5).

As for the PSO, the inertial weight version of the algorithm has been used by setting the control parameters [28] as follows: linearly decreasing 'inertial weight' $w = w_{\max} - k_P\left[\frac{w_{\max} - w_{\min}}{K}\right]$, $w_{\max} = 0.9$ and $w_{\min} = 0.4$, maximum number of iterations $K = 200$, convergence threshold $\eta = 10^{-1}$, 'cognitive acceleration' coefficient (C_1) and 'social acceleration' coefficient (C_2) equal to $C_1 = C_2 = 2.0$ and swarm size proportional to the number of unknowns, $U = 2 \times P$. At the initialisation, the structure of the parasitic array has been randomly chosen within the

Table 2 'Antenna geometry' ($P = 3$) – PSO-optimised descriptors of the parasitic array

Index	Position (λ)		Length (λ)
p	Δy	x_p	h_p
3–4	0.1035	± 0.3553	0.6120
2–5	0.1035	± 0.7224	0.6739
1–6	0.1035	± 1.2366	0.9382

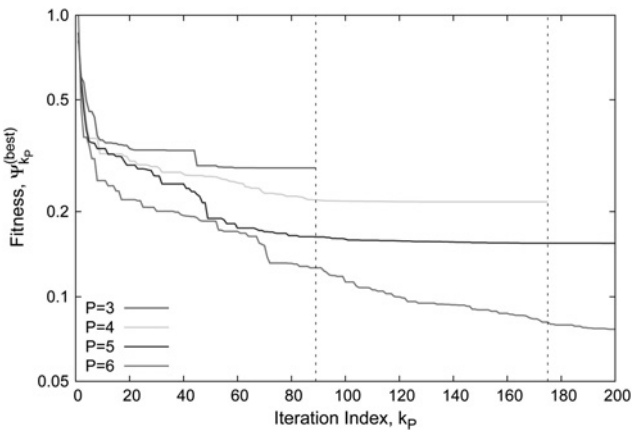

Fig. 8 *Cost function – $P \in [3, 6]$ – behaviour of $\Psi\left(\underline{S}_{k_P}^{(best)}\right)$ against the iteration number, k_p*

following ranges: $h_p/\lambda \in [0.1, 1.0]$ [Such a choice guarantees that each partition of a dipole of the parasitic array (i.e. $h_p/4$, $p = 1,\ldots, P$) is smaller than $h_p/4 < \lambda/4$. Therefore the effect on the field of each dipole (whatever its length h_p) is negligible when turning-off the RF dipole switches [26, 27].], $\Delta y/\lambda \in [0.3, 1.0]$, $x_p/\lambda \in [0.0, (N-1)d/2]$. These latter intervals have been assumed as the boundaries of the admissible solution space, as well.

The first test case refers to the case of a parasitic structure with six dipoles (i.e. $P = 3$). After $K_P = 89$ iterations, the synthesised geometry is sketched in Fig. 7*a*, whereas the values of the coordinates and the lengths of the passive elements are given in Table 2. As expected, the parasitic dipoles are closer to the centre of the array where the differences between the optimal sum and difference patterns (Fig. 2 against Fig. 4) are more significant and, besides the π phase displacement, a higher perturbation of the sum beam is needed to yield the desired difference pattern. First of all, let us note the correct operation of the antenna in the sum mode as shown in Fig. 7*c* that gives the plot of the sum beam in the presence of the switched-off parasitic array (i.e. each parasitic element subdivided into four equal

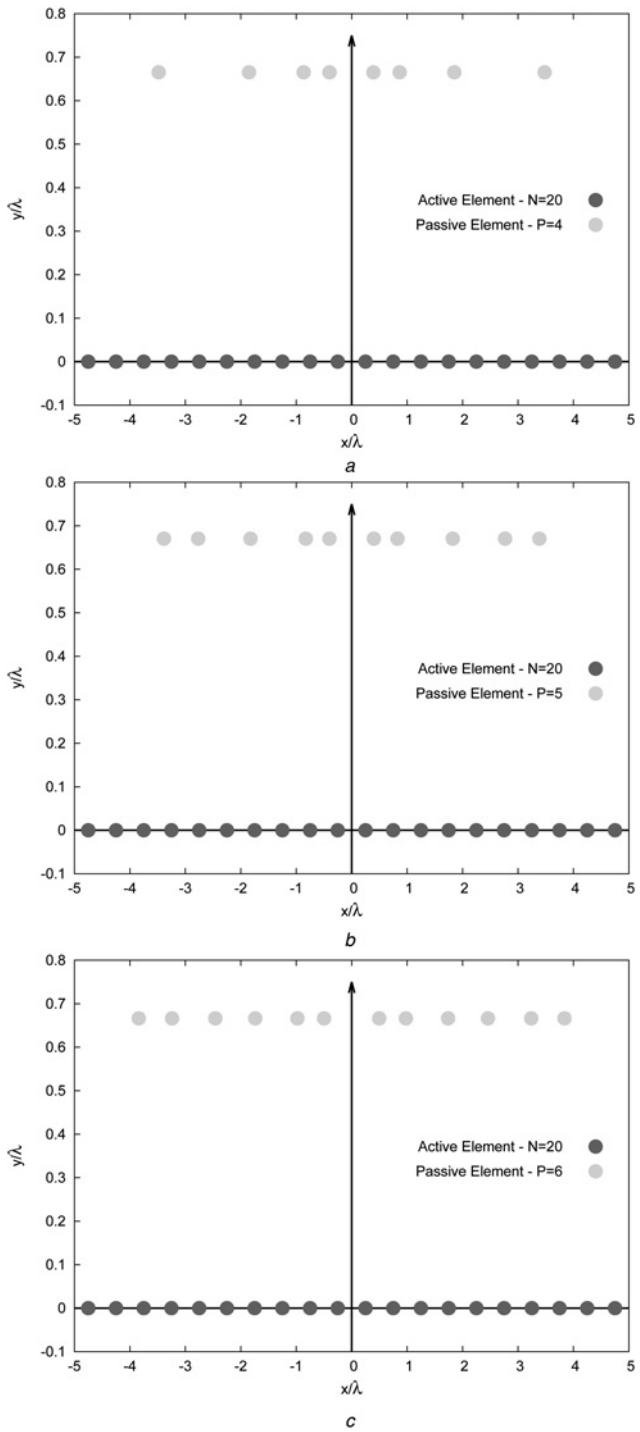

Fig. 9 *Antenna Architectures - PSO-optimised architecture when*
a $P = 4$
b $P = 5$
c $P = 6$

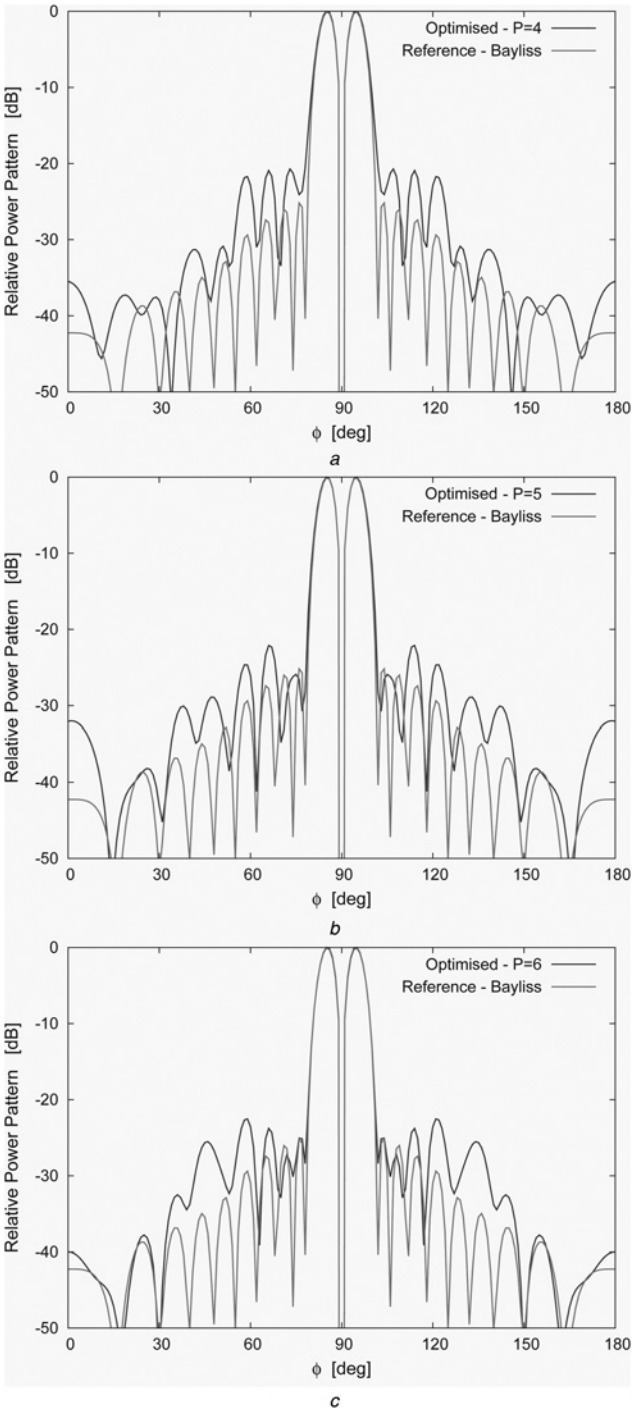

Fig. 10 *Difference patterns – difference pattern radiated by the PSO-optimised architecture when*
a $P = 4$
b $P = 5$
c $P = 6$

doi: 10.1049/iet-rsn.2012.0300

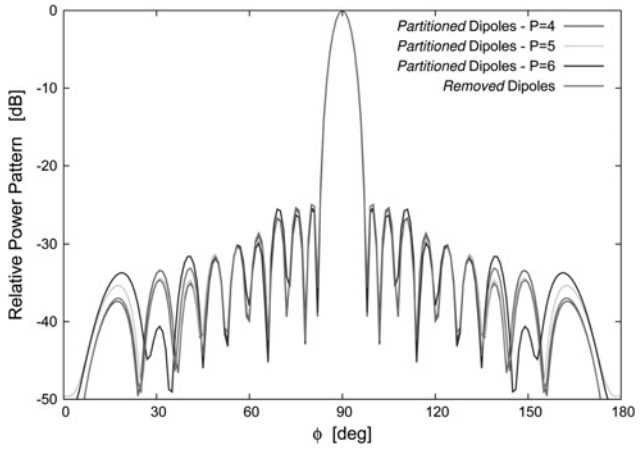

Fig. 11 *Sum patterns – sum pattern radiated by PSO-optimised architecture when P = 4, P = 5 and P = 6*

segments by switching-off the element RF switches) and without the parasitic dipoles. As a matter of fact, the differences between the two patterns turn out to be almost negligible, thus confirming the reliability of the electronic reconfiguration without the need of mechanically moving/removing the passive elements when switching from the difference to the sum mode.

As for the difference mode, Fig. 7*b* shows the synthesised pattern with the reference one as well as the difference beam generated by only imposing phase reversal to half static excitations. Although the non-negligible improvement with respect to this latter, the optimised difference pattern is far from the reference one as confirmed by the high value of the cost function $\Psi_3^{(\text{best})} = 0.286$ $\left(\Psi_3^{(\text{best})} > \eta\right)$. Therefore the number of parasitic dipoles has been increased until $P = 6$ when finally $\Psi_6^{(\text{best})} = 0.077 < \eta$. The behaviour of the optimal fitness, $\Psi\left(\underline{\boldsymbol{S}}_{k_P}^{(\text{best})}\right)$, throughout the iterative PSO-based optimisation is shown in Fig. 8. As it can be observed that the value of $\Psi_P^{(\text{best})}$ monotonically decreases as P increases; thus indicating that a suitable trade-off between the number of passive dipoles and the matching with the reference difference pattern exists as confirmed by the plots of the difference beams in Fig. 9. Concerning the solution with $P = 6$, it is worth noting that the synthesised difference overlaps the reference one within the main-lobe region thus guaranteeing the same accurate resolution capability to the radar tracking system. Moreover, the sidelobes up to $\phi = 30°$ from boresight are close to those of the optimal pattern.

For completeness, the whole set of sum beams and the optimised array architectures is shown in Figs. 10 and 11 (Table 3), respectively. As for the parasitic structure, it can be observed that the parasitic elements are more distant from the active array ($\Delta y \simeq 0.7\lambda$) than in the case with $P = 3$, but they are still more densely distributed around the centre.

4 Conclusions

In this paper, the synthesis of electronically reconfigurable arrays able to generate a sum and a difference pattern for forward-looking monopulse radars has been addressed. The antenna is composed of two parallel linear arrays, the former made of active dipoles and the latter of passive ones each partitioned in a set of segments by locating along its length some RF switches. The sum pattern has been generated by controlling the excitations of the active elements, while the effects of the parasitic dipoles have been made negligible to the radiated field by switching-off the RF switches. On the other hand, the difference pattern has been yielded by introducing a phase displacement of π to half array and turning-on the parasitic dipoles, whose positions and lengths have been optimised by means of a PSO-based procedure to approximate the optimal difference pattern.

The numerical validation has assessed the effectiveness of the proposed approach in synthesising sum and difference patterns by means of an electronically reconfigurable architecture. As expected, the matching with the reference pattern depends on the number of parasitic elements although not very huge arrangements are needed for enabling satisfactory performances.

Future works, out-of-the-scope of this paper, will be aimed at extending the underlying idea to planar and conformal geometries.

Table 3 'Antenna geometry' ($P \in [4, 6]$) – PSO-optimised descriptors of the parasitic array

Index	Position (λ)		Length (λ)
p	Δy	x_p	h_p
$P = 4$			
4–5	0.6653	± 0.3990	0.5537
3–6	0.6653	± 0.8653	0.6442
2–7	0.6653	± 1.8522	0.4419
1–8	0.6653	± 3.4798	0.4241
$P = 5$			
5–6	0.6705	± 0.4004	0.5901
4–7	0.6705	± 0.8273	0.6467
3–8	0.6705	± 1.8246	0.4201
2–9	0.6705	± 2.7674	0.4071
1–10	0.6705	± 3.3851	0.4430
$P = 6$			
6–7	0.6749	± 0.4977	0.5631
5–8	0.6749	± 0.9782	0.8187
4–9	0.6749	± 1.7393	0.4218
3–10	0.6749	± 2.4595	0.3787
2–11	0.6749	± 3.2396	0.4351
1–12	0.6749	± 3.8388	0.4147

5 References

1 Skolnik, I.M.: 'Radar handbook' (McGraw-Hill, 2008, 3rd edn.)
2 Sherman, S.M.: 'Monopulse principles and techniques' (Artech House, 1984)
3 Grimes, D.M., Grimes, C.A.: 'Cradar – an open-loop extended-monopulse automotive radar', *IEEE Trans. Veh. Technol.*, 1989, **38**, (3), pp. 123–131
4 Hansen, T.B., Oristaglio, M.L.: 'Method for controlling the angular extent of interrogation zones in RFID', *IEEE Antennas Wirel. Propag. Lett.*, 2006, **5**, pp. 134–137
5 Lopez, P., Rodriguez, J.A., Ares, F., Moreno, E.: 'Subarray weighting for difference patterns of monopulse antennas: joint optimization of subarray configurations and weights', *IEEE Trans. Antennas Propag.*, 2001, **49**, (11), pp. 1606–1608
6 D'Urso, M., Isernia, T., Meliado', E.F.: 'An effective hybrid approach for the optimal synthesis of monopulse antennas', *IEEE Trans. Antennas Propag.*, 2007, **55**, (4), pp. 1059–1066
7 Chen, Y., Yang, S., Nie, Z.: 'The application of a modified differential evolution strategy to some array pattern synthesis problems', *IEEE Trans. Antennas Propag.*, 2008, **56**, (7), pp. 1919–1927
8 Manica, L., Rocca, P., Martini, A., Massa, A.: 'An innovative approach based on a tree-searching algorithm for the optimal matching of independently optimum sum and difference excitations', *IEEE Trans. Antennas Propag.*, 2008, **56**, (1), pp. 58–66

9 Rocca, P., Manica, L., Azaro, R., Massa, A.: 'A hybrid approach to the synthesis of subarrayed monopulse linear arrays', *IEEE Trans. Antennas Propag.*, 2009, **57**, (1), pp. 280–283

10 Alvarez, M., Rodriguez, J.A., Ares, F.: 'Synthesising Taylor and Bayliss linear distributions with common aperture tail', *Electron. Lett.*, 2009, **45**, (1), pp. 18–19

11 Morabito, A.F., Rocca, P.: 'Optimal synthesis of sum and difference patterns with arbitrary sidelobes subject to common excitations constraints', *IEEE Antennas Wirel. Propag. Lett.*, 2010, **9**, pp. 623–626

12 Elliott, R.S.: 'Antenna theory and design' (Wiley-Interscience IEEE Press, 2003)

13 Kennedy, J., Eberhart, R.C., Shi, Y.: '*Swarm intelligence*' (Morgan Kaufmann, 2001)

14 Rodriguez, J.A., Trastoy, A., Brégains, J.C., Ares, F., Franceschetti, G.: 'Beam reconfiguration of linear arrays using parasitic elements', *Electron. Lett.*, 2006, **42**, (3), pp. 131–136

15 Taylor, T.T.: 'Design of line-source antennas for narrow beam-width and low side lobes', *Trans. IRE Antennas Propag.*, 1955, **3**, (1), pp. 16–28

16 Bayliss, E.T.: 'Design of monopulse antenna difference patterns with low sidelobes', *Bell Syst. Tech. J.*, 1968, **47**, pp. 623–640

17 Dolph, C.L.: 'A current distribution for broadside arrays which optimises the relationship between beam width and sidelobe level', *Proc. IRE*, 1946, **34**, pp. 335–348

18 Bucci, O.M., Caccavale, L., Isernia, T.: 'Optimal far-field focusing of uniformly spaced arrays subject to arbitrary upper bounds in non-target directions', *IEEE Trans. Antennas Propag.*, 2002, **50**, (11), pp. 1539–1554

19 McNamara, D.A.: 'Discrete n-distributions for difference patterns', *Electron. Lett.*, 1986, **22**, (6), pp. 303–304

20 Bucci, O.M., D'Urso, M., Isernia, T.: 'Optimal synthesis of difference patterns subject to arbitrary sidelobe bounds by using arbitrary array antennas', *IEE Proc. Microw. Antennas Propag.*, 2005, **152**, (3), pp. 129–137

21 Balanis, C.A.: 'Antenna theory: analysis and design' (John Wiley & Sons., 1997)

22 Vescovo, R.: 'Reconfigurability and beam scanning with phase-only control for antenna arrays', *IEEE Trans. Antennas Propag.*, 2008, **56**, (6), pp. 1555–1565

23 Ares, F., Franceschetti, G., Rodriguez, J.A.: 'A simple alternative for beam reconfiguration of array antennas', *Prog. Electromag. Res.*, 2008, **88**, pp. 227–240

24 Hansen, R.C.: 'Formulation of echelon dipole mutual impedance for computer', *IEEE Trans. Antennas Propag.*, 1972, **20**, (6), pp. 780–781

25 Boutayeb, H., Denidni, T.A., Mahdjoubi, K., Tarot, A.-C., Sebak, A.-R., Talbi, L.: 'Analysis and design of a cylindrical EBG-based directive antenna', *IEEE Trans. Antennas Propag.*, 2006, **54**, (1), pp. 211–219

26 Zhang, S., Huff, G.H., Feng, J., Bernhard, J.T.: 'A pattern reconfigurable microstrip parasitic array', *IEEE Trans. Antennas Propag.*, 2004, **52**, (10), pp. 2773–2776

27 Petit, L., Dussopt, L., Laheurte, J.-M.: 'MEMS-switched parasitic-antenna array for radiation pattern diversity', *IEEE Trans. Antennas Propag.*, 2006, **54**, (9), pp. 2624–2631

28 Rocca, P., Benedetti, M., Donelli, M., Franceschini, D., Massa, A.: 'Evolutionary optimization as applied to inverse scattering problems', *Inverse Probl.*, 2009, **24**, pp. 1–41

doi: 10.1049/iet-rsn.2012.0300